J. Shanghai Jiao Tong Univ. (Sci.), 2017, 22(2): 206-215
DOI: 10.1007/s12204-017-1823-7

Hybrid Control of Delay Induced Hopf Bifurcation of Dynamical Small-World Network

DING Dawei[a,b*] (丁大为), *ZHANG Xiaoyun*[b] (张肖芸), *WANG Nian*[a,b*] (王　年), *LIANG Dong*[a,b] (梁　栋)
(a. Key Laboratory of Intelligent Computing and Signal Processing of Ministry of Education;
b. School of Electronics and Information Engineering, Anhui University, Hefei 230039, China)

Abstract: In this paper, we focus on the Hopf bifurcation control of a small-world network model with time-delay. With emphasis on the relationship between the Hopf bifurcation and the time-delay, we investigate the effect of time-delay by choosing it as the bifurcation parameter. By using tools from control and bifurcation theory, it is proved that there exists a critical value of time-delay for the stability of the model. When the time-delay passes through the critical value, the model loses its stability and a Hopf bifurcation occurs. To enhance the stability of the model, we propose an improved hybrid control strategy in which state feedback and parameter perturbation are used. Through linear stability analysis, we show that by adjusting the control parameter properly, the onset of Hopf bifurcation of the controlled model can be delayed or eliminated without changing the equilibrium point of the model. Finally, numerical simulations are given to verify the theoretical analysis.
Key words: Hopf bifurcation, hybrid control, small-world network, bifurcation control
CLC number: O 193　　**Document code:** A

0 Introduction

During the last two decades, networks became a subject which discovers information propagation laws in real world models[1]. A great number of studies on the theory and applications of a complex network have shown its superiority in modeling the real-world model. Recently, the small-world network model proposed by Watts and Strogaz[2], which gathers both the large-clustering and small-distance properties, has been widely used due to its potential in capturing the characteristics of many natural and artificial networks, ranging from the Internet, the World Wide Web, human society, power grids to economic and biological models.

Controlling the large-scale infection and epidemic spread of viruses is one of the most concerned issues in this networking age. For example, the spread of severe acute respiratory syndrome (SARS) in 2003 declared by the World Health Organization in the concluding report led to 8 096 known infected cases and 774 deaths worldwide. The spread of computer viruses and worms on the Internet is another urgent problem. There were more than 3×10^{10} dollars in damage caused by the Email worm, and the entire Internet came to a halt in a very short period given without any countermeasures to control the worms[3]. The wide occurrence of spreading behaviors in the small-world network is an interesting issue to investigate the spreading of viruses, diseases and even disasters in the network.

Modeling the spreading of virus by mathematical equations is an effective way to capture the properties of virus propagation[4]. Because the actual process of virus spreading reflects a small-world characteristic, many small-world network models have been established to mimic the spreading of virus. A linear model of disease spreading in d-dimensional small-world lattices, which reveals that the growth of infection is limited to the network scale, was proposed by Moukarzel[5]. The mathematical model is linear and the response is immediate as there is no time delay. Obviously, the model is not adequate to mimic the real propagation process. Yang[6] extended a more general nonlinear model for total influence volume. In Yang's model, a nonlinear interaction component was added into the infected volume with a constant time delay. A limitation of Yang's model is that the nonlinear interaction does not incorporate the topological difference in the small-world network evolution which is in fact of great influence on the spreading dynamics. In 2004, Li et al.[7] proposed a more general nonlinear

Received date: 2015-05-26
Foundation item: the National Natural Science Foundation of China (Nos. 61201227 and 61172127), and the Natural Science Foundation of Anhui (No. 1208085MF93)
∗**E-mail:** dwding@ahu.edu.cn, wn_xlb@ahu.edu.cn

spreading model based on d-dimensional small-world network model. Taking account of the influence of link-adding probabilities, they added another nonlinear interaction to the model. The local stability and Hopf bifurcations of delay-controlled spreading of the model was further investigated by Li and Wang[8], where the link-adding probability and the nonlinear interaction were proved to be fixing points for the oscillating behaviors.

Time delay represents the infection time between separated nodes. In real infectious network topology, the link lengths between nodes are not always equal, so the time delay varies in the process of infection. It comes naturally to wonder if there is a relationship between the time delay and the Hopf bifurcation and whether different time delay affects the critical value of Hopf bifurcation. If the answer is positive, then fixing the link-adding probability by controlling the time delay is also a feasible method to stabilize bifurcating behaviors. In this paper, we are going to analyze the effect of time delay on bifurcating behaviors in the small-world network model.

To control the oscillating in the small-world model, we design an improved hybrid controller to control Hopf bifurcation for the small-world network model. Some methods can achieve the bifurcation control in most researches[9-12], while some controller designs are purely arbitrary and complex and might destroy the characteristic of original model. In this paper, the problem of bifurcation control is solved by an improved hybrid control strategy. As a fact that the natural equilibrium point of the system might not be calculated by analytic expression in practice, we use a real time state feedback hybrid control strategy to take place of the original one. Thus, bifurcation control not only can be realized in mathematical view but also is feasible in reality.

1 Hopf Bifurcation Analysis in Small-World Network Model

Assume that a disease spreads with constant radial velocity $v = 1$ from an original infection site of a network[7]. The total infected volume $V(t)$ grows as a sphere of radius t and surface $\Gamma_d t^{d-1}$ and the primary sphere hits the end of an added link with probability $2P\Gamma_d t^{d-1}$ per unit time, where d stands for the dimension, P is the link-adding probability (note that $0 < P \leqslant 1$ and the topological structure varies with P) and Γ_d is constant with respect to the shaped factor for newly infected site. The total infected volume satisfies

$$V(t) = \Gamma_d \int_0^t [1 + 2PV(t-\tau-\Delta) - \mu(1+2P)V^2(t-\tau-\Delta)]\mathrm{d}\tau, \quad (1)$$

where Δ is constant with respect to the time-delay for newly infected site; μ is the nonlinear interaction parameter, $\mu > 0$.

Considering the case of $d = 1$ and $\Gamma_d = 1$, the total volume of infected individuals in one-dimensional small-world model is formulated as a nonlinear delayed difference equation:

$$\frac{\mathrm{d}V(t)}{\mathrm{d}t} = 1 + 2PV(t-\delta) - \mu(1+2P)V^2(t-\delta), \quad (2)$$

where δ is a time delay

In the following content, the delay induced Hopf bifurcation and stability criteria in small-world network model are derived by analyzing the corresponding characteristics of linearized equation of the small-world network model (2).

Denote $v(t) = V(t) - V^*$, where V^* is the equilibrium of the model (2) with $V(t) > 0$ and is given by

$$V^* = \frac{P + \sqrt{P^2 + \mu(1+2P)}}{\mu(1+2P)}. \quad (3)$$

Expanding the right side of Eq. (2) into the first and second Taylor series at V^*, we have

$$\dot{v}(t) = b_1 v(t-\delta) + b_2 v^2(t-\delta), \quad (4)$$

where

$$b_1 = -2\sqrt{P^2 + \mu(1+2P)}, \quad (5)$$

$$b_2 = -\mu(1+2P). \quad (6)$$

The linearized equation of Eq. (4) is

$$\dot{v}(t) = b_1 v(t-\delta), \quad (7)$$

and the corresponding characteristic equation is

$$\lambda - b_1 \mathrm{e}^{-\lambda\delta} = 0. \quad (8)$$

Assume that Eq. (8) has a pair of pure imaginary roots $\lambda = \pm \mathrm{i}\omega$ with $\omega > 0$. Inserting them into the characteristic equation and separating the real and imaginary parts yield

$$\left.\begin{aligned} b_1 \cos(\omega\delta) &= 0 \\ \omega + b_1 \sin(\omega\delta) &= 0 \end{aligned}\right\}. \quad (9)$$

Therefore, there is

$$\omega\delta = \frac{(2n+1)\pi}{2}, \quad n = 0, 1, 2, \cdots,$$

and

$$\omega + b_2(-1)^n = 0.$$

The critical value of δ can be deduced as

$$\delta_{\mathrm{c}}(n)=-\frac{(2n+1)\pi}{2b_1},\quad n=0,2,4,\cdots.$$

Then, we determine whether the characteristic equation has roots with positive real parts. Let $\lambda=\alpha\pm\mathrm{i}\omega$ for $\omega>0$ and $\alpha>0$ be a root of Eq. (8), then

$$\left.\begin{aligned}\alpha-b_1\mathrm{e}^{-\alpha\delta}\cos(\omega\delta)=0\\ \omega+b_1\mathrm{e}^{-\alpha\delta}\sin(\omega\delta)=0\end{aligned}\right\}. \tag{10}$$

From the first equation of Eq. (10), we know

$$\frac{(2n+1)\pi}{2}<\omega\delta<\frac{(2n+3)\pi}{2},\quad n=0,2,4,\cdots. \tag{11}$$

From the second equation of Eq. (10), we know

$$\omega\delta<\frac{(2n+1)\pi}{2},\quad n=0,2,4,\cdots. \tag{12}$$

Therefore, Eq. (8) may have roots with positive real parts except for $n=0$, i.e. in the case of

$$\left.\begin{aligned}\delta^*=-\frac{\pi}{2b_1}\\ \omega^*=-b_1\end{aligned}\right\}. \tag{13}$$

However, we still have to prove that the model does not have roots with positive real parts when $\delta<\delta^*$.

Considering $b_2<0$, we get

$$\omega\delta=-\delta b_1\mathrm{e}^{-\alpha\delta}\sin(\omega\delta)<-\delta^*b_1=\frac{\pi}{2},$$

thus $0\leqslant\omega\delta<\pi/2$. Then from Eq. (10), we have

$$\alpha=b_1\mathrm{e}^{-\alpha\delta}\cos(\omega\delta)<0,$$

which contradicts $\alpha>0$ as assumed. Therefore, Eq. (10) has no roots with positive real parts when $\delta<\delta^*$. For all $\delta<\delta^*$, all roots of Eq. (10) have negative real parts, so the equilibrium V^* is asymptotically stable whenever $\delta<\delta^*$.

Next, we check the following transversal condition to verify the onset of Hopf bifurcation:

$$\mathrm{Re}\left(\frac{\mathrm{d}\lambda}{\mathrm{d}\delta}\right)_{\delta=\delta^*}>0. \tag{14}$$

We can get

$$\frac{\mathrm{d}\lambda}{\mathrm{d}\delta}=-\frac{b_1\lambda\mathrm{e}^{-\lambda\delta}}{1+b_1\lambda\mathrm{e}^{-\lambda\delta}}.$$

According to $\lambda=\alpha\pm\mathrm{i}\omega$, we have

$$\mathrm{Re}\left(\frac{\mathrm{d}\lambda}{\mathrm{d}\delta}\right)= -\frac{b_1\mathrm{e}^{-\lambda\delta}[\alpha\cos(\omega\delta)+\omega\sin(\omega\delta)+b_1\delta\alpha\mathrm{e}^{-\lambda\delta}]}{[1+b_1\delta\mathrm{e}^{-\lambda\delta}\cos(\omega\delta)]^2+[b_1\delta\mathrm{e}^{-\lambda\delta}\sin(\omega\delta)]^2}. \tag{15}$$

Substituting $\delta=\delta^*$, $\alpha=0$ and $\omega^*\delta^*=\pi/2$ into Eq. (15), we have

$$\mathrm{Re}\left(\frac{\mathrm{d}\lambda}{\mathrm{d}\delta}\right)_{\delta=\delta^*}=-\frac{b_1\omega^*}{1+(\omega^*\delta^*)^2}=\frac{b_1^2}{1+\pi^2/4}>0.$$

Therefore, the transversal condition is satisfied. When $\delta>\delta^*$, the characteristic Eq. (8) has at least one root with strictly positive real part. That is to say, when $\delta>\delta^*$, the equilibrium point of the model (2) is unstable and a limit cycle bifurcates out from the equilibrium point.

Based on the above analysis, we can get the following theorem by applying the Hopf bifurcation theorem.

Theorem 1 For the small-world network model (2), the following results hold with the critical value $\delta^*=-\dfrac{\pi}{2b_1}$. When $\delta<\delta^*$, the equilibrium point of the model (2) is locally and asymptotically stable. When $\delta=\delta^*$, the model (2) exhibits a Hopf bifurcation. When $\delta>\delta^*$, the equilibrium point of the model (2) is unstable and a limit cycle exists.

2 Bifurcation Control with Hybrid Control Strategy

In this section, we address the problem of bifurcation control through hybrid control strategy. If we can extend the stable range of bifurcation parameter in a nonlinear model, it means the Hopf bifurcation can be delayed (even eliminated) or stabilized to a desired unstable periodic orbit. For this purpose, we design the hybrid controller based on parameter perturbation and state feedback method:

$$\begin{aligned}\frac{\mathrm{d}V(t)}{\mathrm{d}t}=&k[1+2PV(t-\delta)-\\ &\mu(1+2P)V^2(t-\delta)]+\\ &(1-k)[V(t-\delta)-V(t)],\end{aligned} \tag{16}$$

where k is the control parameter, $0<k\leqslant1$. When $k=1$, the controlled model (16) equals the original model (2) and it is easy to prove that the model (16) has the same equilibrium V^* as the model (2). Expanding the right-hand side of the model (16) into the first and second Taylor's series around V^*, we have

$$\dot{v}(t)=a_1v(t-\delta)+a_2v(t)+a_3v^2(t-\delta)+\cdots, \tag{17}$$

where

$$\begin{aligned}&v(t)=V(t)-V^*,\\ &a_1=\frac{\partial}{\partial V(t-\delta)}[\dot{V}(t)]|_{V^*}=\\ &\quad k(2P-2\mu(1+2P)V(t-\delta))|_{V^*}+1-k=\\ &\quad 1-k-2k\sqrt{P^2+\mu(1+2P)},\end{aligned}$$

$$a_2 = \frac{\partial}{\partial V(t)}[\dot{V}(t)]|_{V^*} = k-1,$$
$$a_3 = \frac{\partial^2}{2!\partial V^2(t-\delta)}[\dot{V}(t)]|_{V^*} = \frac{1}{2}k(-2\mu(1+2P))|_{V^*} = -k\mu(1+2P).$$

The linear part of the model (16) is

$$\dot{v}(t) = a_1 v(t-\delta) + a_2 v(t). \tag{18}$$

Its characteristic equation is

$$\lambda - a_2 - a_1 \mathrm{e}^{-\lambda\delta} = 0. \tag{19}$$

Lemma 1 If $0 < \mu \leqslant \dfrac{1}{1+2P}\left[\left(\dfrac{k-1}{k}\right)^2 - P^2\right]$, all the roots of Eq. (19) have negative real parts.

Lemma 2 When $\mu > \dfrac{1}{1+2P}\left[\left(\dfrac{k-1}{k}\right)^2 - P^2\right]$ holds, there exists a critical value δ_0 such that all roots of Eq. (19) have negative real parts when $\delta \in [0, \delta_0]$, and Eq. (19) has at least one root with positive part when $\delta > \delta_0$, where

$$\delta_0 = \frac{1}{\sqrt{a_1^2 - a_2^2}} \arccos\left(-\frac{a_2}{a_1}\right).$$

Note that $0 < k < 1$, then $a_2 = k - 1 < 0$. When $a_1 = 0$, we can get all roots of Eq. (19) $\lambda = a_2 < 0$. When $a_1 \neq 0$, let $\pm\mathrm{i}\omega\,(\omega > 0)$ be a root of Eq. (19). Then after detaching the real and imaginary parts of Eq. (19), we have

$$\left.\begin{aligned} a_2 + a_1\cos(\omega\delta) = 0 \\ \omega + a_1\sin(\omega\delta) = 0 \end{aligned}\right\}. \tag{20}$$

From Eq. (20), we obtain $\omega^2 = a_1^2 - a_2^2$, but it does not hold when $|a_1| < -a_2$. When $a_1 = a_2$, for Eq. (19), there is no pure imaginary root, and obviously $\lambda = 0$ is not its root. Thus, we have the conclusion that all roots of Eq. (19) have negative real parts when $a_1 \in [a_2, -a_2)$. From Eq. (20), $a_1 \in [a_2, -a_2)$ is equivalent to inequality:

$$0 < \mu \leqslant \frac{1}{1+2P}\left[\left(\frac{k-1}{k}\right)^2 - P^2\right].$$

This completes the proof of Lemma 1.

Like the proof of Lemma 4 in Ref. [18], δ_0 is defined as the critical value of time-delay and it is the solution of Eq. (20) when $\omega = \sqrt{a_1^2 - a_2^2}$. If $\mu > \dfrac{1}{1+2P}\left[\left(\dfrac{k-1}{k}\right)^2 - P^2\right]$ holds, it means $a_1 < a_2$; obviously, $(\delta_0, \sqrt{a_1^2 - a_2^2})$ is a solution of Eq. (20) and $\pm\mathrm{i}\sqrt{a_1^2 - a_2^2}$ is a pair of pure imaginary roots of Eq. (19) with $\delta = \delta_0$; δ_0 is the first value of $\delta > 0$ such that Eq. (19) has roots with imaginary parts when $\delta \in [0, \delta_0)$. Let $\lambda(\delta) = \rho(\delta) + \mathrm{i}\omega(\delta)$ be the root of Eq. (19) and satisfy $\rho(\delta_0) = 0$ and $\omega(\delta_0) = \sqrt{a_1^2 - a_2^2}$. Differentiating Eq. (19) with δ, we have

$$\frac{\mathrm{d}\lambda}{\mathrm{d}\delta} = -\frac{a_1\lambda\mathrm{e}^{-\lambda\delta}}{1 + a_1\delta\mathrm{e}^{-\lambda\delta}}, \tag{21}$$
$$\rho'(\delta_0) = \mathrm{Re}\left(\left.\frac{\mathrm{d}\lambda}{\mathrm{d}\delta}\right|_{\delta=\delta_0}\right) = \frac{\omega^2}{(1+a_1\delta_0)^2 + (\omega\delta_0)^2} > 0. \tag{22}$$

Thus, at least one root of Eq. (19) has positive part. Then, Eq. (22) is called the transversality condition which indicates there is a Hopf bifurcation occurring from the bifurcation point. The proof of Lemma 2 is completed.

Theorem 2 For the hybrid control model (16), the following results hold with the control parameter $k \in (0, 1]$. If $0 < \mu \leqslant \dfrac{1}{1+2P}\left[\left(\dfrac{k-1}{k}\right)^2 - P^2\right]$, then the equilibrium point V^* is asymptotically stable for all $\delta \geqslant 0$. If $\mu > \dfrac{1}{1+2P}\left[\left(\dfrac{k-1}{k}\right)^2 - P^2\right]$, then the equilibrium point V^* is conditionally stable depending on the value of time-delay δ: ① when $0 < \delta < \delta_0$, the equilibrium point of the model (16) is locally and asymptotically stable; ② when $\delta = \delta_0$, the model (16) exhibits a Hopf bifurcation; ③ when $\delta > \delta_0$, the equilibrium point of the model (16) is unstable and a limit cycle exists.

3 Direction and Stability of Bifurcating Periodic Solutions of Controlled Model

In this section, the direction of the Hopf bifurcation and the stability of the bifurcating periodic solutions when $\delta = \delta_0$ are analyzed by the center manifold and the normal form theories. One can achieve the stability control through choosing an appropriate value of k. The center manifold and the normal form theories are wildly used in bifurcation analyses, like the method used in Ref. [20]. Here, we omit the specific steps of analysis and give the conclusion directly.

Theorem 3 For the controlled model (16), the Hopf bifurcation is determined by the parameters μ_2, β_2 and τ_2. Specifically, μ_2 determines the direction of the Hopf bifurcation; β_2 determines the stability of the bifurcating periodic solution; τ_2 determines the period of the bifurcating periodic solution. The conclusions are summarized as follows. If $\mu_2 > 0$ ($\mu_2 < 0$), the

Hopf bifurcation is supercritical (subcritical) and the bifurcating periodic solutions exist for $\delta > \delta_0$ ($\delta < \delta_0$). If $\beta_2 < 0$ ($\beta_2 > 0$), the bifurcating periodic solutions are stable (unstable). If $\tau_2 > 0$ ($\tau_2 < 0$), the period increases (decreases).

Definitions of μ_2, τ_2 and β_2 are given as follows:

$$C_1(0) = \frac{\mathrm{i}}{2\omega_0}\left(g_{20}g_{11} - 2|g_{11}|^2 - \frac{1}{3}|g_{02}|^2\right) + \frac{g_{21}}{2},$$
$$\mu_2 = -\frac{\mathrm{Re}\, C_1(0)}{\mathrm{Re}\, \lambda'(0)},$$
$$\tau_2 = -\frac{\mathrm{Im}\, C_1(0) + \mu_2 \mathrm{Im}\, \lambda'(0)}{\omega_0},$$
$$\beta_2 = 2\mathrm{Re}\, C_1(0),$$

where

$$g_{20} = g_{02} = -g_{11} = -2\bar{B}\bar{P},$$
$$g_{21} = 2\bar{B}\mathrm{i}\Big(\bar{P}\frac{g_{20} + g_{02} + 2\bar{P}}{\bar{P} - 2\mathrm{i}\omega_0} - 4g_{11} + 4\bar{P}\Big),$$
$$\bar{B} = \frac{1}{1 + \delta_0 \mathrm{e}^{-\mathrm{i}\omega_0\delta_0}\bar{P}},$$
$$\bar{P} = 1 - k - 2k\sqrt{P^2 + \mu(1+2P)},$$
$$\omega_0 = \frac{1}{\delta_0}\arccos\left(-\frac{a_2}{a_1}\right),$$
$$\delta_0 = \frac{1}{\sqrt{a_1^2 - a_2^2}}\arccos\left(-\frac{a_2}{a_1}\right).$$

As a result, all parameters can be obtained by the parameters in the model (16) and the conclusions are shown in Theorem 3.

4 Numerical Simulations

4.1 Delay Induced Bifurcation in Small-World Network Model

In this section, we present numerical results to verify the analytic conclusions obtained in the previous derivation in Section 1, and analyze the stability of the delay induced bifurcation of the small-world network model without control.

For a consistent comparison, here we select $\mu = 0.8$ as used in Ref. [9]. Based on Eq. (13), we can conclude the relation between P and δ^*. The result is shown in Fig. 1.

As mentioned in Ref. [9], the characteristics of small world are more obvious when the newly adding probability is set as $0 < P \ll 1$. For this reason, we conduct experiments on two situations of $P = 0.01$ and $P = 0.1$.

Figure 2 shows the waveform plots and phase portraits of the small-world network model (2) corresponding to different time-delay δ. Clearly, the delay induced Hopf bifurcation follows the conclusion of Theorem 1.

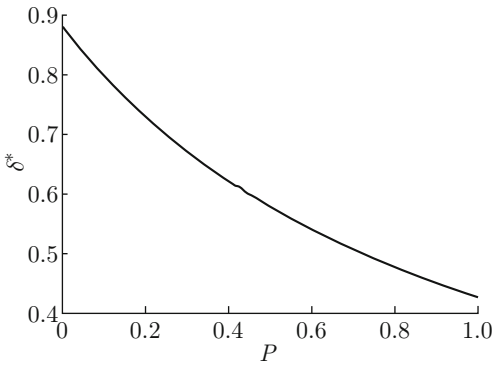

Fig. 1 The curve of P versus δ^*

When $\delta = 0.6 < \delta^*$, the model (2) is asymptotically stable, as shown in Fig. 2(a); when $\delta = 0.79 = \delta^*$, the model (2) exhibits a Hopf bifurcation, as shown in Fig. 2(b); when $\delta = 1 > \delta^*$, the equilibrium point of the model (2) is unstable and a limit cycle exists, as shown in Fig. 2(c).

When $P = 0.1$ and $\mu = 0.8$, based on Eq. (13), we compute $\delta^* = 0.79$. Figure 3 shows the corresponding bifurcating diagram of the small-world network model (2). As we can see, there exists a critical value of time-delay δ^*, and a Hopf bifurcation occurs from the equilibrium point V^* when $\delta = \delta^*$. Figure 3 proves that the time-delay is related to the oscillation behaviors of the model.

When $P = 0.01$ and $\mu = 0.8$, based on Eq. (13), we compute $\delta^* = 0.87$. Figure 4 shows the corresponding bifurcating diagram. As shown in Fig. 4, there exists a Hopf bifurcation when the time-delay goes though the critical value δ^*.

In turn, we set $\delta = 0.8$, $\delta = 0.87$ and $\delta = 1$. When $\delta = 0.8 < \delta^*$, the model (2) is asymptotically stable, as shown in Fig. 5(a); when $\delta = 0.79 = \delta^*$, the model (2) exhibits a Hopf bifurcation, as shown in Fig. 5(b); when $\delta = 1 > \delta^*$, the equilibrium point of the model (2) is unstable and a limit cycle exists, as shown in Fig. 5(c).

Besides, here we select $P = 0.1$ as used in Ref. [9]. Based on Eq. (13), the relation between μ and δ^* is obtained. The result is shown in Fig. 6. As shown in Fig. 6, the stable region for time delay δ reduces with the increase of the nonlinear factor μ.

As analyzed in the above and previous works, the general spreading dynamical behavior in small-world network depends on many factors, such as reaction speed δ, topological structure P and nonlinearity μ. In Fig. 7, we plot the plane in the first quadrant of (μ, p, δ^*) space which divides the stable region and the unstable region with the marks D_2 and D_1, respectively. It is noted that when the parameters are chosen under the plane, the model is stable.

Figure 8 shows the bifurcation diagrams corresponding to $\mu = 0.2$, 0.4, 0.6, 0.8.

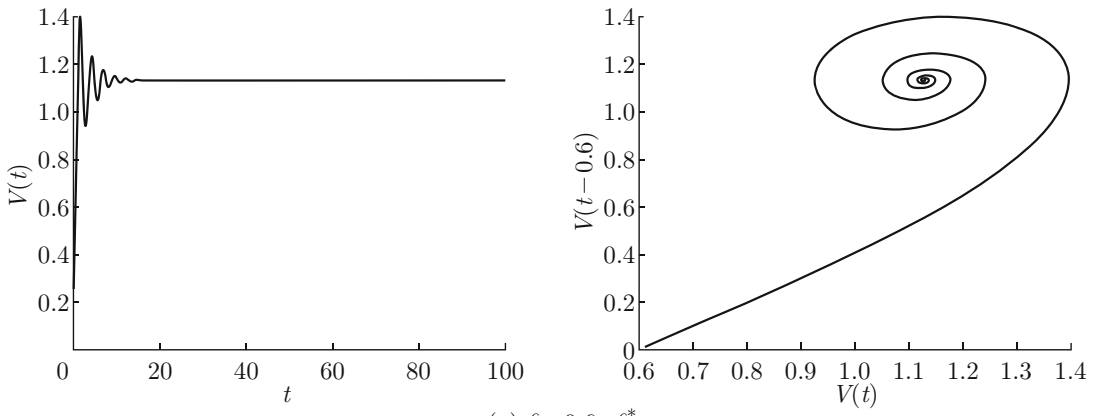

(a) $\delta=0.6<\delta^*$

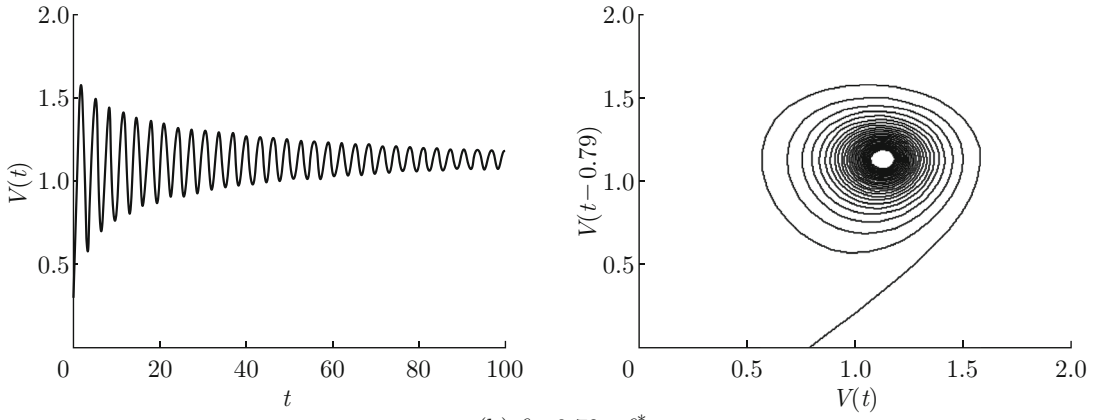

(b) $\delta=0.79=\delta^*$

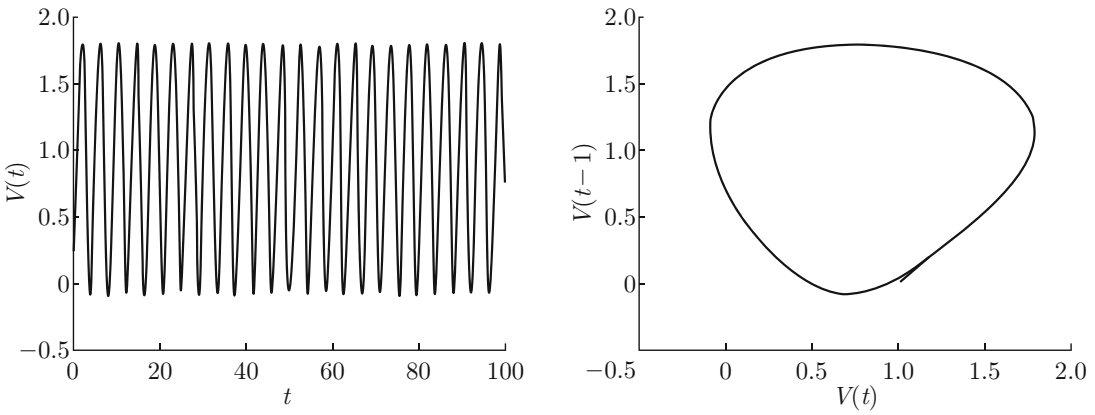

(c) $\delta=1>\delta^*$

Fig. 2 The waveform plots and phase portraits of the model (2) with $P = 0.1$ and $\mu = 0.8$

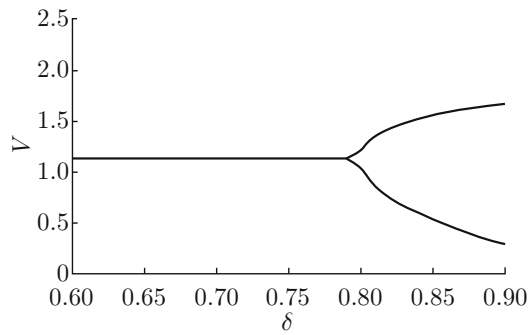

Fig. 3 The bifurcation diagram of the model (2) with $P = 0.1$ and $\mu = 0.8$

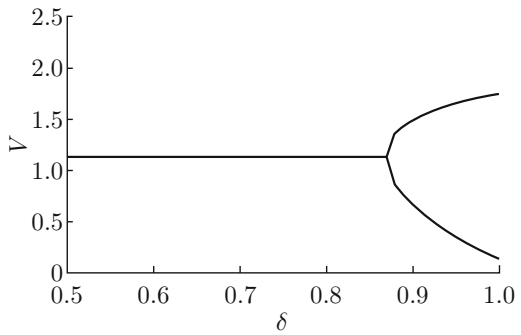

Fig. 4 The bifurcation diagram of the model (2) with $P = 0.01$ and $\mu = 0.8$

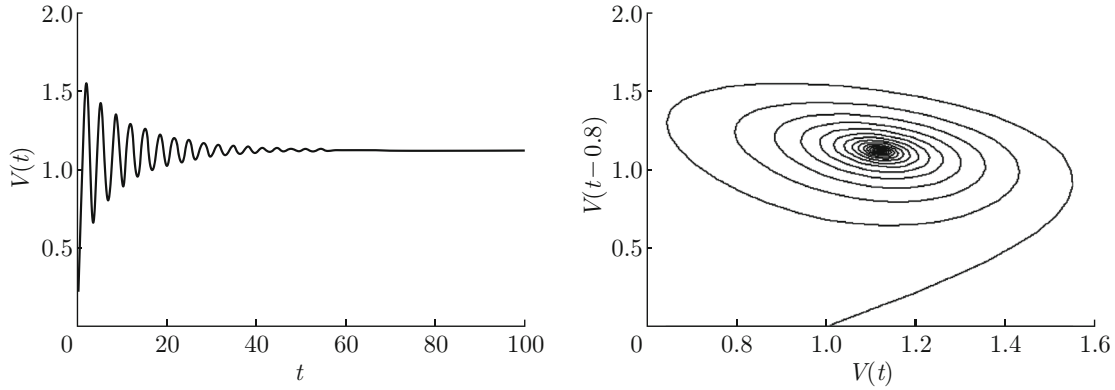

(a) $\delta=0.8<1$

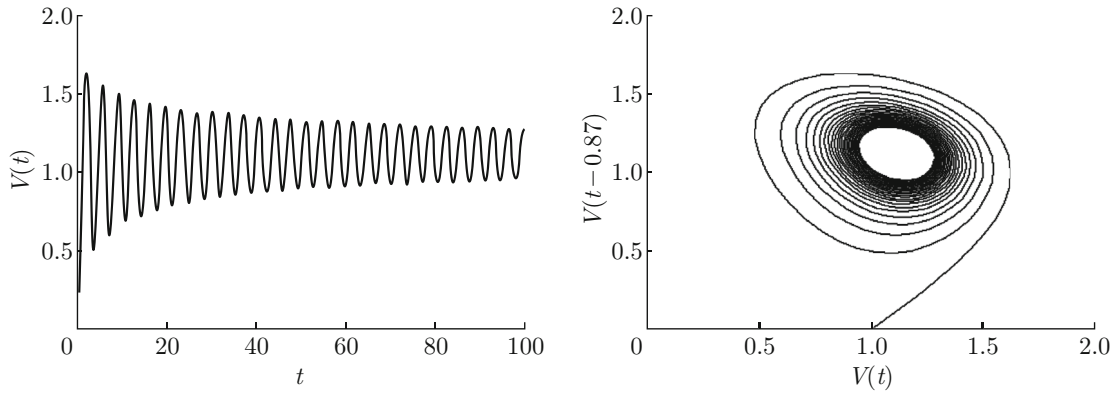

(b) $\delta=0.87=\delta^*$

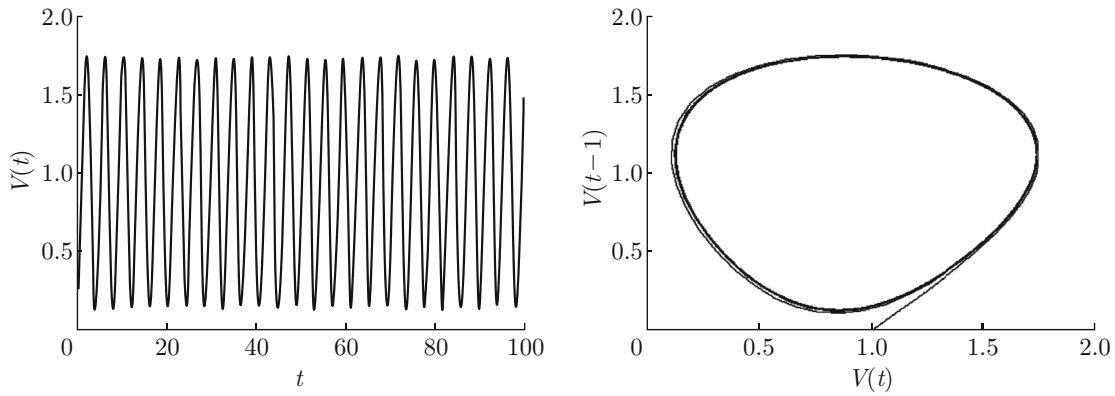

(c) $\delta=1>\delta^*$

Fig. 5 The waveform plots and phase portraits of the model (2) with $P=0.01$ and $\mu=0.8$

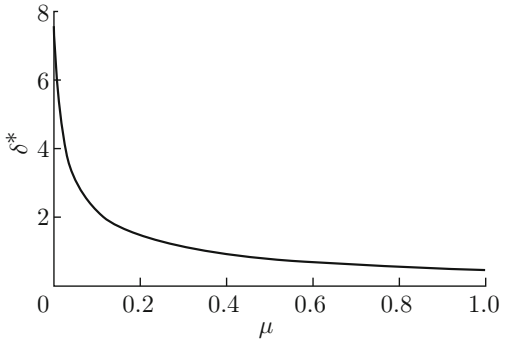

Fig. 6 The curve of μ versus δ^*

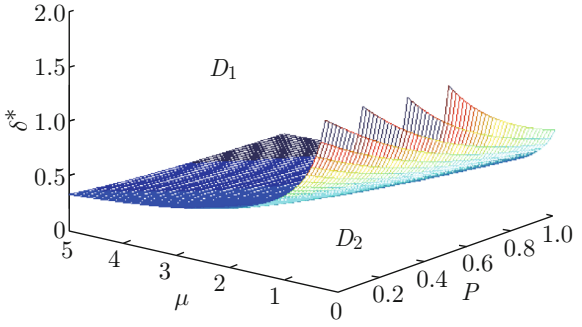

Fig. 7 The plane of $\delta^*=\pi/[4\sqrt{P^2+\mu(1+2P)}]$

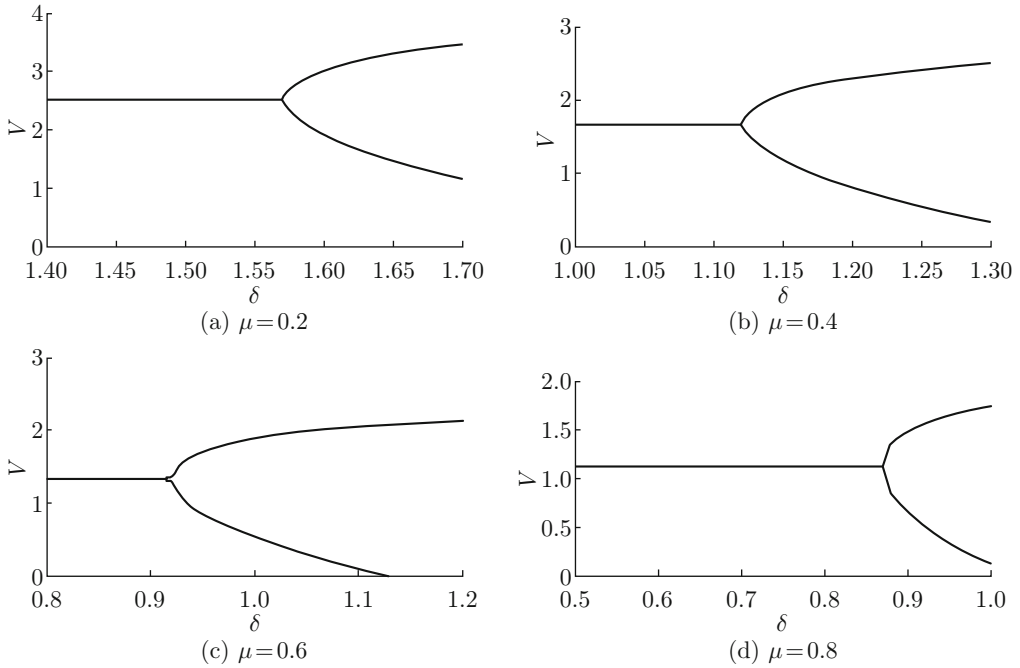

Fig. 8 The bifurcation diagrams of the model (2) with different μ and $P = 0.1$

4.2 Hopf Bifurcations in Small-World Network Model with Hybrid Control

In this section, we present the numerical simulations and verify the performance of the hybrid control strategy to control the Hopf bifurcation in the small world network model (16). For consistent comparison with the original model, we set $P = 0.1$ and the control parameter $k \in (0, 1]$.

As shown in Fig. 9, the curve of μ versus k divides the first quadrant into two regions: S_1 and S_2. From Theorem 2, S_2 is absolutely stable and S_1 is conditionally stable.

For consistent comparison, we set $\mu = 0.8$ and $P = 0.1$, which means $\mu \in S_1$. In other words, the model is conditional stable, depending on the value of δ. As shown in Fig. 10, the curve δ_0 versus k divides the first quadrant into two regions: R_1 and R_2. As concluded in Theorem 2, when $\mu \in S_1$, R_2 is the stable region and R_1 is the unstable region.

Figure 11 shows the waveform plots and phase portraits of the small world network model (16) with hybrid control. To verify Theorem 2, we first set the parameter $P = 0.1$ for control parameter $k = 0.6$. From Figs. 9 and 10, $\mu = 0.365$ and $\delta_0 = 3.171$ are obtained. In the condition of $\mu = 1 > \mu_0$ i.e. $\mu \in S_1$, from Theorem 2, there are 3 cases: when $\delta < \delta_0$, the model (16) is conditionally stable; when $\delta = 4 > \delta_0$, the model is unstable and a Hopf bifurcation occurs, as shown in Fig. 11(a); when $\delta = 2 < \delta_0$, the model is asymptotic stable, as shown in Fig. 11(b). Besides, when $\mu = 0.2 < \mu_0$ i.e. $\mu \in S_2$, the model is absolute stable; no matter how the time-delay δ changes, the

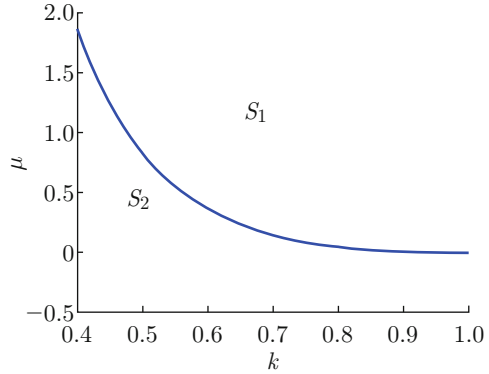

Fig. 9 The curve of μ versus k

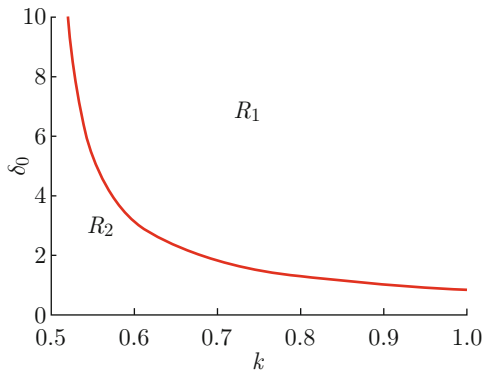

Fig. 10 The curve of δ_0 versus k

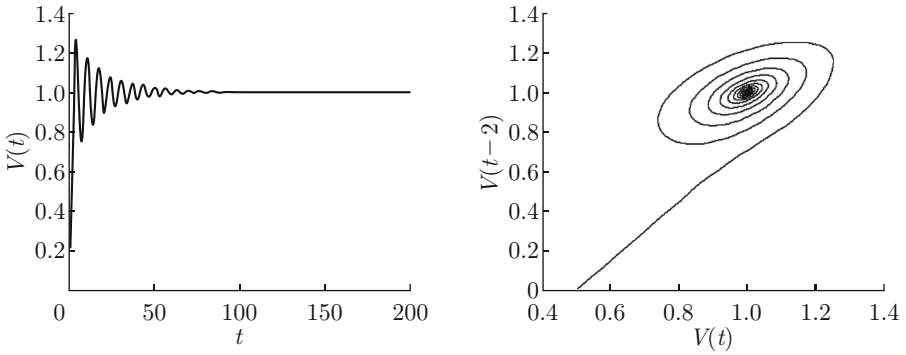

(a) $\mu=1$, $\delta=2$

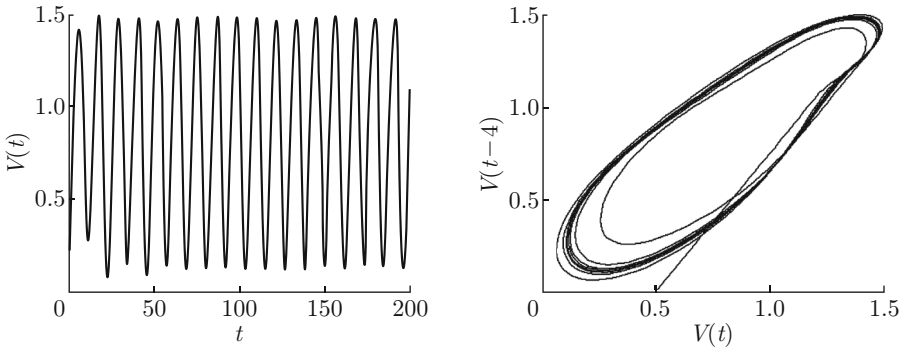

(b) $\mu=1$, $\delta=4$

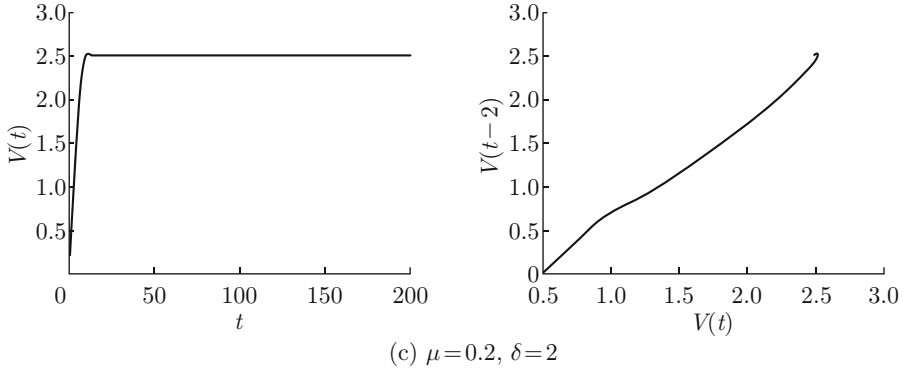

(c) $\mu=0.2$, $\delta=2$

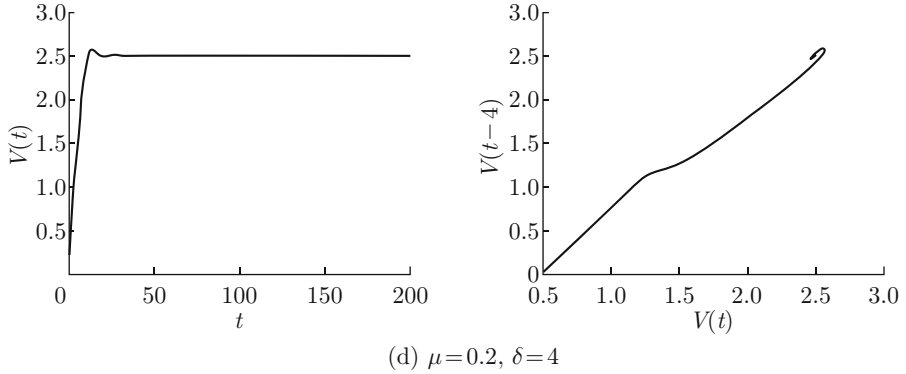

(d) $\mu=0.2$, $\delta=4$

Fig. 11 The waveform plots and phase portraits of the stable model (16)

model will remain stable, as shown in Figs. 11(c) and 11(d).

It is noted from above analysis that when μ is set as a constant, the critical value δ_0 increases as the control parameter k grows. Therefore, one can extend the stable region of the small-world network model by choosing a proper control parameter. To verify the performance of the hybrid strategy as a comparison with respect to

Fig. 5, we simulate the controlled model (16) by setting parameters of $P = 0.1$, $\mu = 0.8$, $\delta = 1$ and $k = 0.8$. The results shown in Figs. 12 and 13 indicate that the bifurcation has been successfully delayed. It is noted that the bifurcation can even be eliminated by adjusting the control parameter properly.

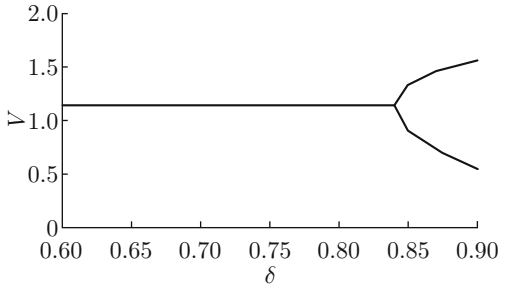

Fig. 12 The bifurcation diagram of the model (16) with $P = 0.1$, $\mu = 0.8$, $\delta = 1$ and $k = 0.8$

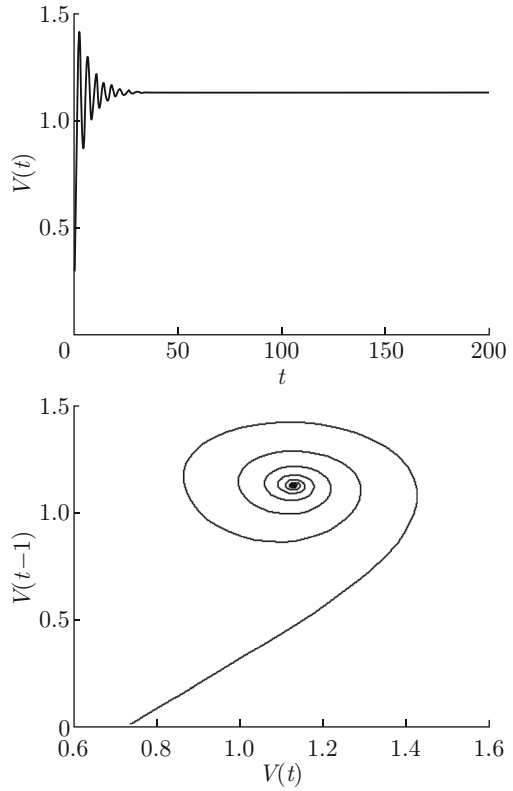

Fig. 13 The waveform plot and phase portrait of the model (16) with $P = 0.1$, $\mu = 0.8$, $\delta = 1$ and $k = 0.8$

5 Conclusion

The stability analysis and Hopf bifurcation control of a small-world network are concerned in this paper. Based on the tools from control and bifurcation theory, it can be concluded that the critical value of the small-world network model varies when we change the system parameters (such as, nonlinear factor, topology and communication delay). Moreover, a hybrid controller based on state feedback and parameter perturbation is proposed to delay the onset of Hopf bifurcation of the model. Theoretical analysis shows that the hybrid control can successfully expand the stable region of the model. Finally, the validity of theoretical conclusions is demonstrated by numerical examples.

References

[1] BARABÁSI A L, ALBERT R, JEONG H. Mean field theory for scale free random graph [J]. *Physica A: Statistical Mechanics and Its Applications*, 1999, **272**(1): 173-187.

[2] WATTS D J, STROGAZ S H. Collective dynamics of small-world network [J]. *Nature*, 1998, **393**(6684): 440-442.

[3] BAO Z J, JIANG Q Y, YAN W J, et al. Stability of the spreading in small-world network with predictive controller [J]. *Physics Letters A*, 2010, **374**(13): 1560-1564.

[4] MENG M, LI S, MA H R. The transition of epidemic spreading in small world [J]. *Journal of Shanghai Jiao Tong University*, 2006, **40**(5): 869-972 (in Chinese).

[5] MOUKARZEL C F. Spreading and shortest paths in systems with sparse long-range connections [J]. *Physical Review E*, 1999, **60**(6): 6263-6266.

[6] YANG X S. Fractals in small-world network with time-delay [J]. *Chaos, Solitons and Fractals*, 2002, **13**(2): 215-219.

[7] LI X, CHEN G R, LI C G. Stability and bifurcation of disease spreading in complex networks [J]. *International Journal of Systems Science*, 2004, **35**(9): 527-536.

[8] LI X, WANG X F. Controlling the spreading in small-world evolving networks: Stability, oscillation, and topology [J]. *IEEE Transactions on Automatic Control*, 2006, **51**(3): 534-540.

[9] XIAO M, HO D W C, CAO J D. Time-delayed feedback control of dynamical small-world network at Hopf bifurcation [J]. *Nonlinear Dynamics*, 2009, **58**(1/2): 319-344.

[10] XU C, ZHOU Y L, WANG Y. Control of Hopf bifurcation in a fluid-flow model in wireless networks [J]. *Journal of Shanghai Jiao Tong University*, 2014, **48**(10): 1479-1484 (in Chinese).

[11] CHENG Z S, CAO J D. Hybrid control of Hopf bifurcation in complex networks with delays [J]. *Neurocomputing*, 2014, **131**: 164-170.

[12] DING D W, ZHU J, LUO X S, et al. Delay induced Hopf bifurcation in a dual model of Internet congestion control algorithm [J]. *Nonlinear Analysis: Real World Applications*, 2009, **10**(5): 2873-2883.